

論文 / 著書情報
Article / Book Information

Title	Hydrogen Limits Carbon in Liquid Iron
Author(s)	Kei Hirose, Shoh Tagawa, Yasuhiro Kuwayama, Ryosuke Sinmyo, Guillaume Morard, Yasuo Ohishi, Hidenori Genda
Citation	Geophysical Research Letters, Vol. 46, Issue 10, pp. 5190-5197
Pub. date	2019, 5
Copyright	An edited version of this paper was published by AGU. Copyright 2019 American Geophysical Union.
DOI	https://doi.org/10.1029/2019GL082591

Geophysical Research Letters

RESEARCH LETTER

10.1029/2019GL082591

Key Points:

- Melting experiments on the Fe-C-H system were performed to 127 GPa
- Hydrogen limits the solubility of carbon in liquid iron
- Melting temperature of FeH_x ($x > 1$) is about 2380 K at 135 GPa, lower than those of Fe alloyed with the other possible core light elements

Supporting Information:

- Supporting Information S1

Correspondence to:

K. Hirose,
kei@elsi.jp

Citation:

Hirose, K., Tagawa, S., Kuwayama, Y., Sinmyo, R., Morard, G., Ohishi, Y., & Genda, H. (2019). Hydrogen limits carbon in liquid iron. *Geophysical Research Letters*, 46, 5190–5197. <https://doi.org/10.1029/2019GL082591>





Received 25 FEB 2019

Accepted 28 APR 2019

Accepted article online 6 MAY 2019

Published online 22 MAY 2019

Hydrogen Limits Carbon in Liquid Iron

Kei Hirose^{1,2} , Shoh Tagawa² , Yasuhiro Kuwayama², Ryosuke Sinmyo², Guillaume Morard³ , Yasuo Ohishi⁴, and Hidenori Genda¹ 

¹Earth-Life Science Institute, Tokyo Institute of Technology, Tokyo, Japan, ²Department of Earth and Planetary Science, The University of Tokyo, Tokyo, Japan, ³Sorbonne Université, Muséum National d'Histoire Naturelle, UMR CNRS 7590, Institut de Minéralogie, de Physique des Matériaux et de Cosmochimie, IMPMC, Paris, France, ⁴Japan Synchrotron Radiation Research Institute, Hyogo, Japan

Abstract Melting experiments were performed on the Fe-C-H system to 127 GPa in a laser-heated diamond anvil cell. On the basis of in situ and ex situ sample characterizations, we found that the solubility of carbon in liquid Fe correlates inversely with hydrogen concentration at ~60 GPa and ~3500 K, indicating that liquid Fe preferentially incorporates hydrogen rather than carbon under conditions with abundant C and H. While large amounts of both C and H may have been delivered to the growing Earth, C-poor/H-rich metals were likely added to the protocore in the late stages of core formation. We also obtained a melting curve of FeH_x ($x > 1$) far beyond the pressure range in earlier determinations. Its liquidus temperature was found to be 2380 K at 135 GPa, lower than those of Fe alloyed with the other possible core light elements. Relatively low core temperature is thus supported by the presence of hydrogen.

Plain Language Summary Both carbon and hydrogen are possible major light elements in the core but estimation of their abundance in the core as well as in the bulk Earth is difficult because of their high volatility. In addition, the property of hydrogen-bearing iron alloys has been the least studied. Here we performed melting experiments on Fe-C-H to 127 GPa, close to the pressure at the top of the Earth's core. Our main finding is that hydrogen limits the solubility of carbon in liquid Fe; the carbon content correlates inversely with hydrogen concentration in molten Fe coexisting with diamonds at ~60 GPa and ~3500 K. Recent planet formation theories suggest that large amounts of C and H were delivered to the growing Earth. In the late stages of core formation, liquid metals preferentially incorporating hydrogen rather than carbon may have added to the protocore. We also found that hydrogen decreases the melting temperature of Fe remarkably. The melting temperature of FeH_x ($x > 1$) is only about 2380 K at the core-mantle boundary; lower than those of Fe-Fe₃S eutectic and Fe alloyed with the other possible core light elements.

1. Introduction

The light elements in the Earth's core still remain unknown and could be a combination of silicon, oxygen, sulfur, carbon, and hydrogen (Poirier, 1994). According to recent planet formation theories, it is likely that both C and H (as organic materials and hydrous minerals) were delivered to the growing Earth. Early migration of Jupiter and Saturn in the “Grand Tack Model” (Walsh et al., 2011) caused radial mixing between volatile-poor materials formed in the terrestrial planet region and volatile-rich materials (such as carbonaceous chondrites) formed in the outer region, which provided C and H to the Earth's building blocks. The falling of centimeter- to meter-sized pebbles toward the Sun in the protoplanetary disk, examined in the “Pebble Accretion Model” (e.g., Sato et al., 2016), also delivers C and H to the terrestrial planet region. Therefore, interaction of this C and H with Fe metals may be an inevitable process during Earth's core formation. While Fe-C and Fe-H alloys have been the least studied among possible core alloys (see Figure 1 in Hirose et al., 2013), previous first-principle calculations suggested that both the density and velocity of the outer core are reconciled with liquid Fe-H (Umemoto & Hirose, 2015). Recent calculations also found that carbon could be an important impurity element in the solid inner core as it decreases the shear velocity of solid Fe substantially (Li et al., 2018).

The previous metal-silicate partitioning experiments by Clesi et al. (2018) and Malavergne et al. (2019) argued that hydrogen is least partitioned into molten iron. However, they found at most only ~500 ppm H in quenched molten Fe, because the vast majority of hydrogen had been lost during decompression. The solubility of hydrogen in solid Fe is $H/Fe = <10^{-5}$ at ambient condition (see Figure. 1 in Fukai & Suzuki,

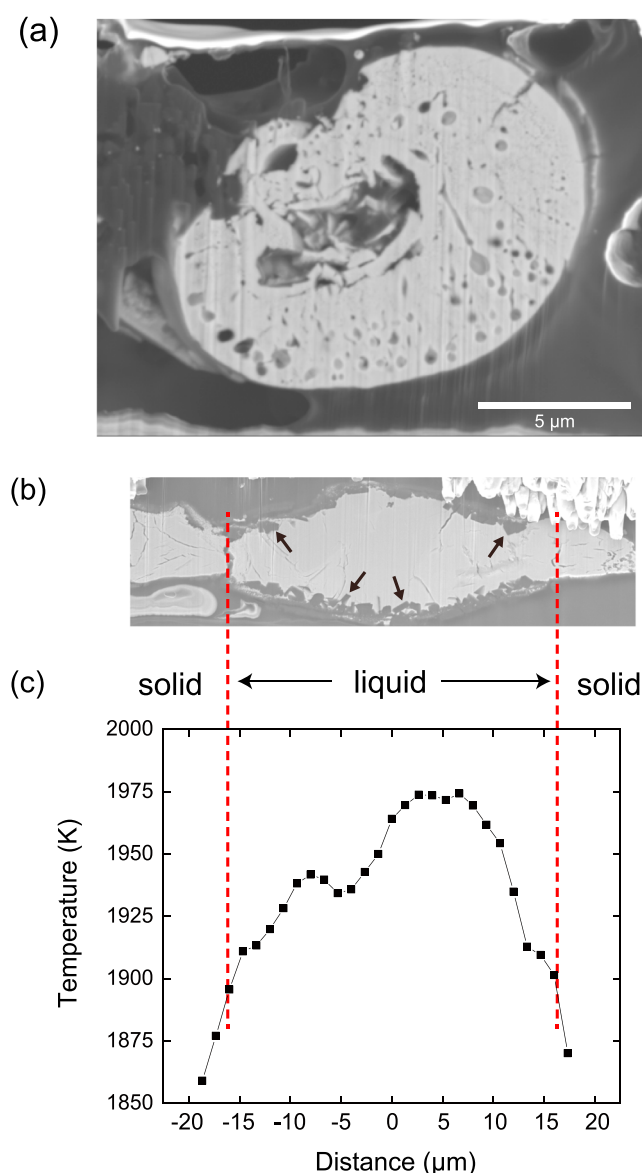


Figure 1. Sample cross sections from runs (a) #1 and (b) #4. Quenched molten Fe is surrounded by diamonds; see arrows for euhedral crystals that formed in iron in (b). Bubbles and cracks found in the iron were formed when hydrogen escaped during decompression. Temperature at the liquid-solid boundary is given in (c), considering identical temperature for both sides.

1986). It has been repeatedly reported that hydrogen goes away from solid Fe when it transforms into the body-centered cubic phase upon decompression (Iizuka-Oku et al., 2017; Okuchi, 1997). The melting temperature in the Fe-H system is similar to that of pure Fe at 1 bar (Fukai et al., 2003), which means that hydrogen is neither soluble in solid nor liquid Fe at ambient pressure and therefore indicates that hydrogen originally included in iron under high pressure escapes during pressure release.

The property of liquid Fe-C has been well examined at high pressures (e.g., Fei & Brosh, 2014; Morard et al., 2017; Nakajima et al., 2015). In contrast, earlier experiments on Fe-H alloys are limited even for solids (e.g., Fukai, 1992; Pépin et al., 2014), in particular at high temperatures (Fukai et al., 2003; Sakamaki et al., 2009; Terasaki et al., 2012). While Terasaki et al. (2014) reported that solid Fe_3C does not incorporate hydrogen at 14 GPa, Narygina et al. (2011) demonstrated that Fe_3C was once formed from Fe + $\text{C}_n\text{H}_{2n+2}$ paraffin and then replaced by FeH + C diamond at >1600 K and 54 GPa (Ohta et al., 2018; Thompson et al., 2018). These results indicate that (1) carbon and hydrogen do not coexist in solid Fe and (2) hydrogen is more siderophile than carbon at relatively high pressure and temperature (P - T).

Some combinations of light elements are mutually exclusive in liquid Fe as well. Liquid-liquid immiscibility was observed in a variety of iron alloy systems such as Fe-S-O (Urakawa et al., 1987) and Fe-Si-S (Sanloup & Fei, 2004). In addition, strong interactions between light elements limit their simultaneous solubilities in liquid Fe, for example, between Si and O (Hirose et al., 2017; O'Neill et al., 1998). The solubility of C in liquid Fe (carbon concentration in liquid Fe coexisting with graphite) is known to diminish with increasing Si content (Li et al., 2015; Takahashi et al., 2013).

In addition, it has been argued that the incorporation of hydrogen reduces the melting temperature of Fe remarkably and it is therefore compatible with relatively low core temperatures (Nomura et al., 2014). The melting curve of Fe-H, however, has been determined only up to 20 GPa (Sakamaki et al., 2009; Shibazaki et al., 2014), and its extrapolation to the core pressure range includes a lot of uncertainty.

In this study, we examined the solubility of carbon in liquid Fe-H by changing the hydrogen and carbon concentrations at 58–66 GPa and ~3500 K, close to a typical P - T condition for metal-silicate segregation in a single-stage core formation model (Fischer et al., 2015; Siebert et al., 2013). Our results demonstrate that liquid Fe incorporates hydrogen preferentially when both C and H are present. Furthermore, we also determined the melting curve of FeH_x ($x > 1$) to 127 GPa, showing its low melting temperature compared to iron alloyed with the other possible core light elements.

2. Experimental Methods

High P - T experiments were carried out in a laser-heated diamond anvil cell (DAC) using 300- μm flat and 120- μm beveled diamond anvils. We loaded a foil or a ~10- μm sphere of pure Fe (>99.9% purity, Wako) between the $\text{C}_n\text{H}_{2n+2}$ paraffin or $\text{C}_{14}\text{H}_{10}$ phenanthrene layers in a hole at the center of a preindented rhenium gasket (Table 1). Both paraffin and phenanthrene were employed as sources of carbon and hydrogen; the latter provides less hydrogen upon heating. In run #3, in order to increase the C/H ratio of the system, we employed a 5- μm piece of a homogeneous Fe+4.0wt% C sample prepared by an ultra-rapid quenching method (Morard et al., 2017) and a mixture of Al_2O_3 powder + paraffin as a pressure medium.

Table 1
Experimental Results

Run #	Sample	Medium	<i>P</i> (GPa)	<i>T</i> (K)	H (wt%) ^a	H (wt%) ^b	C (wt%)	Liq. composition
1	Fe sphere	Paraffin (C _n H _{2n+2})	60	3710	1.8	1.5	0.5(2)	Fe _{0.49} C _{0.01} H _{0.50}
2	Fe sphere	Phenanthrene (C ₁₄ H ₁₀) ^c	66	3220	1.0	0.8	1.0(2)	Fe _{0.62} C _{0.03} H _{0.35}
3	Fe + 4 wt% C chip	Paraffin + Al ₂ O ₃ mixture	58	3650	0.7	0.6	3.6(2)	Fe _{0.63} C _{0.11} H _{0.26}
4	Fe foil	Paraffin	43	1900	not measured	not measured	not measured	
5	Fe foil	Paraffin	68	<2100	2.9	2.4	0.2(1)	Fe _{0.37} H _{0.63} (FeH _{1.67}) ^d
6	Fe foil	Paraffin	108	2260	1.8	1.5		Fe _{0.49} H _{0.51} (FeH _{1.02}) ^d
7	Fe foil	Paraffin	127	<2120	4.0	3.1	0.3(1)	Fe _{0.30} H _{0.70} (FeH _{2.33}) ^d

^aBased on ΔV_H from Caracas (2015). ^bFrom Fukai (1992). ^cPhenanthrene layer + Al₂O₃ layer. ^dAssuming no carbon.

After loading, a whole DAC was put into a vacuum desiccator overnight, and subsequently, the sample chamber was flushed with dry argon and squeezed in an argon atmosphere.

After compression to a pressure of interest, the sample was heated from both sides with a couple of 100 W single-mode Yb fiber lasers. A laser beam was converted to one with a flat energy distribution by beam-shaping optics, which diminishes the radial temperature gradient. The laser-heated spot was 20–30 μm across, which was larger than the entire iron and alloy samples in runs #1–#3 (Figure 1a). The heating duration was limited to 3 s in order to avoid temperature fluctuation, which is long enough for carbon and hydrogen to diffuse over an entire liquid pool (Helffrich, 2014). Considering that the melting/crystallization of coexisting diamonds (see diamond crystals grown in molten iron in Figure 1b) occurred almost instantaneously and carbon concentration was homogeneous in the quenched liquid pool, chemical equilibrium between the liquid metal and coexisting diamonds should have been attained.

A 1-D temperature distribution was obtained using a spectro-radiometric method (Figure 1c). Two types of experiments were performed in this study. First, we examined the solubility of carbon with changing hydrogen concentration in liquid Fe coexisting with diamonds (runs #1–#3) at 58–66 GPa and 3220–3710 K, which is above the melting temperature of pure Fe. The entire Fe-C-H samples (5- to 15- μm size) were fully molten in these experiments (Figure 1a). Second, we determined the melting curve of FeH_x ($x > 1$; runs #4–#7) at 43–127 GPa and 1900–2260 K. In runs #4 and #6, only a part of the sample was molten, and thus, the temperature at the boundary between liquid and solid gives a melting (liquidus) temperature (Figures 1b and 1c), which is the upper bound for a eutectic temperature. The entire sample was melted in runs #5 and #7, for which we show the lowest temperature in the sample that represents the upper limit for a liquidus temperature.

Pressure was measured after heating at 300 K based on the Raman shift of diamond (anvil; Akahama & Kawamura, 2004). The contribution of thermal pressure was then corrected (Andrault et al., 1998); for purely isochoric heating, the thermal pressure is written as $\Delta\alpha K_T \times T$, where α is thermal expansivity and K_T is isothermal bulk modulus. We employed $\alpha K_T = 4$ MPa/K and 60% of the theoretical value by following Morard et al. (2011). Such a thermal pressure estimate is indeed consistent with the empirical one assuming a 5% pressure increase with each temperature increase of 1000 K (Fiquet et al., 2010; Nomura et al., 2014); the differences are within ± 1 GPa in runs #1–#5 and ± 4 –6 GPa in runs #6–#7. The overall errors in temperature and pressure may be $\pm 5\%$ and $\pm 10\%$, respectively, according to Mori et al. (2017).

In situ high *P-T* X-ray diffraction (XRD) measurements were performed at BL10XU, SPring-8 for all experiments except run #4. Angle-dispersive XRD spectra were collected on a flat panel detector (Perkin Elmer) sequentially every 200 ms during heating. A monochromatic incident X-ray beam was collimated to 6 μm (full width at half maximum). Since hydrogen escapes from solid Fe during decompression to 1 bar (Fukai & Suzuki, 1986; Iizuka-Oku et al., 2017; Okuchi, 1997), hydrogen concentration in quenched liquid alloy was estimated from the volume of FeH_x at high pressure and 300 K, which appeared upon quenching temperature (Figure S1 in the supporting information). The hydrogen content, x in FeH_x, can be obtained

$$x = (V_{\text{FeH}_x} - V_{\text{Fe}}) / \Delta V_H \quad (1)$$

in which V_{Fe} is the volume of Fe (Dewaele et al., 2006) and ΔV_H is the volume increase per hydrogen atom. Table 1 gives the hydrogen contents when employing the ΔV_H by Caracas (2015; from his

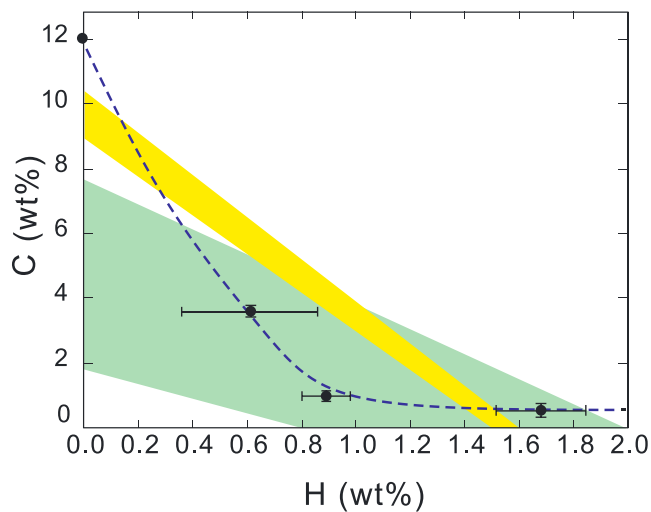


Figure 2. Solubility of carbon in liquid Fe-H (carbon concentration in liquid coexisting with diamond) as a function of the hydrogen content (the average between the lowest and the highest estimates) examined at 58–66 GPa and 3220–3710 K. Data for hydrogen-free condition (50 GPa and 3500 K) is from Fei and Brosh (2014). Previously proposed possible Fe-C-H liquid core compositions are shown by the green region. The yellow band gives the possible compositional range for a projectile core, which was originally formed under both C- and H-rich environments and added to the Earth's protocore forming the stratified layer at its top. See text for details.

calculations with $x = 1.0$) and Fukai (1992) that give the highest and the lowest values, respectively (ΔV_H can be estimated also from Pépin et al., 2014). When such quench crystals were annealed by laser at ~ 1500 K and 65 GPa, we found that the hydrogen content decreased only slightly from $x = 1.21$ to 1.14. Considering hydrogen diffuses fast, such hydrogen content after thermal annealing should represent the bulk hydrogen concentration in quenched molten iron, which is indeed similar to that found in quench crystals. It verifies the present determination of hydrogen concentration in molten Fe. The liquid obtained in run #3 contained 3.6 wt% C, and solid Fe formed from it could have contained up to 1 wt% C (Fei & Brosh, 2014; Mashino et al., 2019). Carbon is incorporated into solid Fe by both substituting Fe atoms and occupying interstitial sites, which reduces and expands the volume of Fe, respectively (Huang et al., 2005; Li et al., 2018). The maximum effect of carbon on the estimate of hydrogen concentration in liquid Fe in run #3 is calculated to be ± 0.2 wt% H (Figure 2).

We performed textural and chemical characterizations on recovered samples. A cross section of a laser-heated portion of the sample was obtained parallel to the compression axis by using a Focused Ion Beam (FIB, FEI Versa™ 3D DualBeam™). It was examined by a field emission (FE)-type scanning electron microscope and energy dispersive X-ray spectrometry for elemental mapping. The carbon contents in quenched liquid iron were then determined using an FE-type electron probe micro-analyzer (FE-EPMA, JEOL JXA-

8530F) with a voltage of 12 kV and a beam current of 15 nA. We used Fe and Fe_3C as standards and LIF (Fe) and LDE2H (C) as analyzing crystals. The carbon concentration in quenched molten iron was obtained by subtracting 0.25–0.37 wt% C that was detected inside of the rhenium gaskets, which is believed to be contamination that occurred during FIB processing and EPMA analysis.

3. Results

Microprobe observations of recovered samples show small bubbles and cracks in the iron (Figure 1), indicating that hydrogen was originally included in the iron but escaped during decompression to 1 bar (Okuchi, 1997). We also found that the solubility of carbon in liquid iron (carbon concentration in molten iron coexisting with diamond) is limited to less than 0.5 wt% when the liquid includes a relatively large amount of hydrogen (FeH_x , $x > 1$; Table 1).

The entire iron and alloy samples were heated in runs #1–#3 (Figure 1a). During heating, the XRD peaks from solid iron were lost, while those of diamond appeared (Figure S1 in the supporting information). The lattice volume of iron that formed upon temperature quench was larger than that of original pure iron, indicating that the liquid contained 0.7 to 1.8 wt% H when using the ΔV_H from Caracas (2015). Observations of sample cross sections found that quenched liquid alloy coexisted with diamonds (see Figure 1b), which is consistent with the XRD observations and shows that the system was saturated with carbon. Melting of the sample in runs #5–#7 was also confirmed by the XRD patterns collected at high P - T (Figure S2 in the supporting information). For run #4, melting is indicated by the formation of euhedral, relatively large crystals of diamond within Fe-H alloy.

We found that the carbon contents in these liquids are limited compared to those of the Fe-C binary liquids that coexist with diamonds (Figure 2). The thermodynamic model by Fei and Brosh (2014) on the Fe-C binary system indicates that liquid coexisting with diamond at 50 GPa and 3500 K includes 12 wt% C. It suggests that the solubility of carbon in molten iron at 58–66 GPa and ~ 3500 K decreases substantially with increasing hydrogen concentration, from ~ 12 wt% C without hydrogen ($\text{Fe}_{0.61}\text{C}_{0.39}$) to 3.6 ± 0.2 wt% C with 0.6 ± 0.2 wt% H ($\text{Fe}_{0.63}\text{C}_{0.11}\text{H}_{0.26}$) and 0.5 ± 0.2 wt% C with 1.7 ± 0.2 wt% H ($\text{Fe}_{0.49}\text{C}_{0.01}\text{H}_{0.50}$).

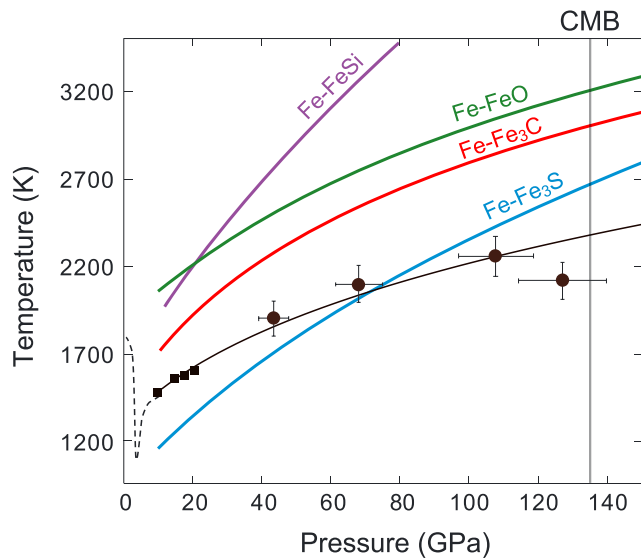


Figure 3. Melting temperatures of FeH_x . Black curve represents the melting curve for FeH_x ($1 < x < 2$). Liquid at 127 GPa included more hydrogen ($x > 2$). Broken line is from Fukai et al. (2003) and Sakamaki et al. (2009). Data are fitted by Simon-Glatzel equation; $T_{\text{melting}} = T_0 [(P_{\text{melting}} - P_0)/a + 1]^{1/c}$, $a = 24.6$, $c = 3.8$, and $T_0 = 1473$ K and $P_0 = 9.5$ GPa (Sakamaki et al., 2009). Melting temperatures of FeH_x are lower than those of eutectic melting in $\text{Fe-Fe}_3\text{S}$ and of the other binary Fe alloys at the CMB.

The present microprobe analyses showed only 0.2–0.3 wt% C in hydrogen-rich liquid Fe in runs #5 and #7, which is consistent with our findings described above. The liquids found in runs #5–#7 are therefore Fe-H binary liquids in practice (most likely in run #4 as well; Table 1). Therefore, on the basis of their melting temperatures, the melting curve for FeH_x ($x > 1$) was obtained to 127 GPa (Figure 3), close to the conditions at the core-mantle boundary (CMB).

4. Discussion

4.1. Hydrogen Limits the Solubility of Carbon in Liquid Iron

Earlier DAC experiments above 50 GPa on the solid Fe-C-H system demonstrated a sequence of reactions, $\text{Fe} + \text{C}_n\text{H}_{2n+2} \rightarrow 2\text{Fe}_3\text{C} + 3\text{H}_2 \rightarrow 6\text{FeH} + 2\text{C}$ with increasing temperature (Narygina et al., 2011; Ohta et al., 2018), indicating that hydrogen dismisses carbon from solid iron at high temperatures (e.g., >1650 K at 54 GPa). The present study performed at 43–127 GPa shows that hydrogen limits the solubility of carbon not only in solid iron but also in liquid iron (Figure 2). In solids, both carbon and hydrogen atoms occupy interstitial sites in a close-packed iron lattice, while the other candidate core light elements substitute for iron atoms (carbon does both). It is likely that the hydrogen atom is smaller than the carbon one and can thus preferentially occupy the interstitial sites. This may be applied for liquids as well, leading to preferential incorporation of hydrogen over carbon in molten iron at the lower-mantle pressure range.

Runs #1–#3 were carried out at 58–66 GPa and 3220–3710 K, close to the conditions for metal-silicate segregation leading to Earth's core formation (Fischer et al., 2015; Siebert et al., 2013). Since the giant impact is a stochastic event (e.g., Kokubo & Genda, 2010), it is possible that the impactor that was responsible for the last, Moon-forming giant impact had been formed in the volatile-rich outer region of the solar system. If this is the case, both C and H could be the important core impurity elements. Nevertheless, the solubility of carbon in liquid Fe-H determined by the present experiments gives the maximum concentration of carbon in core-forming metals, depending on their hydrogen abundance. Assuming carbon is a sole light element, 1.8–7.7 wt% C has been proposed to account for the outer core density and sound velocity (Sata et al., 2010; Badro et al., 2014; Nakajima et al., 2015; Morard et al., 2017). Experimental and theoretical studies demonstrated that they are also reconciled with 0.8–2.0 wt% H in molten iron (Terasaki et al., 2012; Thompson et al., 2018; Umemoto & Hirose, 2015). The green region in Figure 2 shows the possible compositional range of the Fe-C-H liquid core supposed from these studies. Indeed, a part of the green region includes carbon more than the solubility curve, and such area is therefore unlikely to represent the outer core composition.

More realistically the Earth's core formation was not a single-stage event. Landeau et al. (2016) argued that the stratified layer atop the core could have been formed by the merging of a lighter projectile core and the Earth's protocore following a giant impact. They estimated that the projectile core was originally 3.8%–5.0% less dense than the Earth's protocore; the density being that much smaller than that of the topmost outer core is explained by the presence of 8.9–10.4 wt% C or 1.5–1.6 wt% H in liquid iron based on the calculations at the CMB conditions (Badro et al., 2014; Umemoto & Hirose, 2015). Such an Fe-C-H projectile core composition is represented by the yellow region in Figure 2. Most of the yellow region includes carbon more than the solubility curve and is therefore not viable, leaving the possibility of a C-rich/H-poor or C-poor/H-rich projectile core. Indeed, the former is unlikely since the projectile core should have preferentially incorporated hydrogen rather than carbon under both C- and H-rich conditions.

4.2. Low Melting Temperature of Fe-H Alloy

We obtained the melting temperatures of FeH_x ($x > 1$) to 127 GPa, close to the pressure at the CMB (Table 1), which extends the previous determinations by Sakamaki et al. (2009) up to 20 GPa. Our data show that the liquidus temperatures of $\text{FeH}_{1.02}$ and $\text{FeH}_{2.33}$ are 2260 ± 110 K at 108 GPa and $<2120 \pm 110$ K at 127 GPa,

respectively, lower than the 2500 K at 108 GPa for the eutectic melting in Fe-Fe₃S (Mori et al., 2017) and much lower than those of the other binary iron alloys, Fe-Si (Fischer et al., 2013), Fe-O (Morard et al., 2017), and Fe-C (Mashino et al., 2019; Figure 3). If we do not consider the data at 127 GPa because the liquid was enriched in hydrogen more than FeH₂, that is, an Fe-H intermediate compound stable above 67 GPa (Pépin et al., 2014), the liquidus temperature between FeH and FeH₂ is about 2380 K at the CMB.

The lowermost mantle is not globally molten. Ultralow velocity zones may represent partially molten areas above the CMB, but they are only observed locally. It suggests that the temperature at the CMB should not exceed the solidus temperature of a representative mantle material (e.g., pyrolite), which has been determined to be $\sim 4150 \pm 150$ K from XRD data (Andrault et al., 2011; Fiquet et al., 2010) or 3570 ± 200 K in the presence of ~ 400 ppm water based on chemical characterizations of recovered samples (Nomura et al., 2014). Moreover, it is noted that if the present-day CMB temperature is close to the solidus temperature of the representative lowermost mantle material, the mantle side of the CMB is supposed to have been extensively molten in the recent past; the core cooling rate can be 100 K/Gyr (Hirose et al., 2017) but can also be as high as >300 K/Gyr (Labrosse, 2015). At the same time, the liquidus temperature of the alloy comprising the Earth's outer core must be lower than the CMB temperature. Our experiments support the notion that, in order for the outer core to be fully molten even under relatively low CMB temperature, hydrogen is present in the outer core.

5. Conclusion

We have performed melting experiments on the Fe-C-H system to 127 GPa in a laser-heated DAC, combined with in situ synchrotron XRD measurements and ex situ textural and chemical characterizations on sample cross sections. The results demonstrate that hydrogen limits the solubility of carbon in liquid Fe; molten Fe contains about 12 wt% C when hydrogen is absent (Fei & Brosh, 2014), while it includes only 0.5 wt% C with 1.8 wt% H (Fe_{0.49}C_{0.01}H_{0.50}) at 60 GPa and 3710 K. Earlier experiments have reported that a sequence of reactions, $\text{Fe} + \text{C}_n\text{H}_{2n+2} \rightarrow 2\text{Fe}_3\text{C} + 3\text{H}_2 \rightarrow 6\text{FeH} + 2\text{C}$, occur with increasing temperature above 50 GPa (Narygina et al., 2011; Ohta et al., 2018), indicating that hydrogen expels carbon from solid iron. Our experiments show that it occurs in liquid as well.

Earth's building blocks that accreted in the late stages of planet formation were likely to have been enriched in both C and H. Our findings suggest that at such late stages, core-forming metals preferentially incorporate hydrogen with a minimal amount of carbon under C- and H-rich conditions. Such liquid metals may have been lighter than the preexisting Earth's protocore and might have formed a stratified layer atop the core as observed seismologically today (Landeau et al., 2016).

The hydrogen-rich liquid iron obtained in this study included <0.5 wt% C, and therefore, their melting temperatures practically represent those for liquid FeH_x ($x > 1$). Their melting curve was determined to 127 GPa, much higher than the pressure range in the earlier determinations by Sakamaki et al. (2009) up to 20 GPa. The melting temperature of FeH_x ($1 < x < 2$) is found to be about 2380 K at the CMB, lower than those in the Fe-Fe₃S and the other binary iron alloy systems. The incorporation of hydrogen reduces the melting temperature of Fe to a large extent, which is helpful for the outer core to be fully molten even under relatively low core temperatures.

Acknowledgments

Data for Figures 2 and 3 are given in Table 1. Synchrotron XRD measurements were performed at BL10XU, SPring-8 (proposal numbers 2018A0072 and 2018B0072). This work was supported by JSPS Kakenhi 16H06285. K. Yonemitsu is acknowledged for her FIB/SEM/EDS/EPMA analyses. Comments from anonymous reviewers helped improve the manuscript.

References

- Akahama, Y., & Kawamura, H. (2004). High-pressure Raman spectroscopy of diamond anvils to 250 GPa: Method for pressure determination in the multimegabar pressure range. *Journal of Applied Physics*, 96(7), 3748–3751. <https://doi.org/10.1063/1.1778482>
- Andrault, D., Bolfan-Casanova, N., Lo Nigro, G., Bouhifd, M. A., Garbarino, G., & Mezouar, M. (2011). Solidus and liquidus profiles of chondritic mantle: Implication for melting of the Earth across its history. *Earth and Planetary Science Letters*, 304(1–2), 251–259. <https://doi.org/10.1016/j.epsl.2011.02.006>
- Andrault, D., Fiquet, G., Itié, J. P., Richet, P., Gillet, P., Hausermann, D., & Hanfland, M. (1998). Thermal pressure in the laser-heated diamond-anvil cell: An X-ray diffraction study. *European Journal of Mineralogy*, 10(5), 931–940. <https://doi.org/10.1127/ejm/10/5/0931>
- Badro, J., Cote, A. S., & Brodholt, J. P. (2014). A seismologically consistent compositional model of Earth's core. *Proceedings of the National Academy of Sciences USA*, 111(21), 7542–7545. <https://doi.org/10.1073/pnas.1316708111>
- Caracas, R. (2015). The influence of hydrogen on the seismic properties of solid iron. *Geophysical Research Letters*, 42, 3780–3785. <https://doi.org/10.1002/2015GL063478>
- Clesi, V., Bouhifd, M. A., Bolfan-Casanova, N., Manthilake, G., Schiavi, F., Raepsaet, C., et al. (2018). Low hydrogen contents in the cores of terrestrial planets. *Science Advances*, 4(3). <https://doi.org/10.1126/sciadv.1701876>

- Dewaele, A., Loubeyre, P., Occelli, F., Mezouar, M., Dorogokupets, P. I., & Torrent, M. (2006). Quasihydrostatic equation of state of iron above 2 Mbar. *Physical Review Letters*, 97, 29–32. <https://doi.org/10.1103/PhysRevLett.97.215504>
- Fei, Y., & Brosh, E. (2014). Experimental study and thermodynamic calculations of phase relations in the Fe–C system at high pressure. *Earth and Planetary Science Letters*, 408, 155–162. <https://doi.org/10.1016/j.epsl.2014.09.044>
- Fiquet, G., Auzende, A. L., Siebert, J., Corgne, A., Bureau, H., Ozawa, H., & Garbarino, G. (2010). Melting of peridotite to 140 gigapascals. *Science*, 329(5998), 1516–1518. <https://doi.org/10.1126/science.1192448>
- Fischer, R. A., Campbell, A. J., Reaman, D. M., Miller, N. A., Heinz, D. L., Dera, P., & Prakapenka, V. B. (2013). Phase relations in the Fe–FeSi system at high pressures and temperatures. *Earth and Planetary Science Letters*, 373, 54–64. <https://doi.org/10.1016/j.epsl.2013.04.035>
- Fischer, R. A., Nakajima, Y., Campbell, A. J., Frost, D. J., Harries, D., Langenhorst, F., et al. (2015). High pressure metal–silicate partitioning of Ni, Co, V, Cr, Si, and O. *Geochimica et Cosmochimica Acta*, 167, 177–194. <https://doi.org/10.1016/j.gca.2015.06.026>
- Fukai, Y. (1992). Some properties of the Fe–H system at high pressures and temperatures, and their implications for the Earth's core. In Y. Syono & M. H. Manghnani (Eds.), *High Pressure Research: Application to Earth and Planetary Sciences* (pp. 373–385). Tokyo: TERRAPUB.
- Fukai, Y., Mori, K., & Shinomiya, H. (2003). The phase diagram and superabundant vacancy formation in Fe–H alloys under high hydrogen pressures. *Journal of Alloys and Compounds*, 348(1–2), 105–109. [https://doi.org/10.1016/S0925-8388\(02\)00806-X](https://doi.org/10.1016/S0925-8388(02)00806-X)
- Fukai, Y., & Suzuki, T. (1986). Iron–water reaction under high pressure and its implication in the evolution of the Earth. *Journal of Geophysical Research*, 91(B9), 9222–9230. <https://doi.org/10.1029/JB091iB09p09222>
- Helffrich, G. (2014). Outer core compositional layering and constraints on core liquid transport properties. *Earth and Planetary Science Letters*, 391, 256–262. <https://doi.org/10.1016/j.epsl.2014.01.039>
- Hirose, K., Labrosse, S., & Hernlund, J. (2013). Composition and state of the core. *Annual Review of Earth and Planetary Sciences*, 41(1), 657–691. <https://doi.org/10.1146/annurev-earth-050212-124007>
- Hirose, K., Morard, G., Sinmyo, R., Umemoto, K., Hernlund, J., Helffrich, G., & Labrosse, S. (2017). Crystallization of silicon dioxide and compositional evolution of the Earth's core. *Nature*, 543(7643), 99–102. <https://doi.org/10.1038/nature21367>
- Huang, L., Skorodumova, N. V., Belonoshko, A. B., Johansson, B., & Ahuja, R. (2005). Carbon in iron phases under high pressure. *Geophysical Research Letters*, 32, L21314. <https://doi.org/10.1029/2005GL024187>
- Iizuka-Oku, R., Yagi, T., Gotou, H., Okuchi, T., Hattori, T., & Sano-Furukawa, A. (2017). Hydrogenation of iron in the early stage of Earth's evolution. *Nature Communications*, 8, 14096. <https://doi.org/10.1038/ncomms14096>
- Kokubo, E., & Genda, H. (2010). Formation of terrestrial planets from protoplanets under a realistic accretion condition. *The Astrophysical Journal Letters*, 714(1), L21–L25. <https://doi.org/10.1088/2041-8205/714/1/L21>
- Labrosse, S. (2015). Thermal evolution of the core with a high thermal conductivity. *Physics of the Earth and Planetary Interiors*, 247, 36–55. <https://doi.org/10.1016/j.pepi.2015.02.002>
- Landeau, M., Olson, P., Deguen, R., & Hirsh, B. H. (2016). Core merging and stratification following giant impact. *Nature Geoscience*, 9(10), 786–789. <https://doi.org/10.1038/NGEO2808>
- Li, Y., Dasgupta, R., & Tsuno, K. (2015). The effects of sulfur, silicon, water, and oxygen fugacity on carbon solubility and partitioning in Fe-rich alloy and silicate melt systems at 3 GPa and 1600 °C: Implications for core–mantle differentiation and degassing of magma oceans and reduced planetary mantles. *Earth and Planetary Science Letters*, 415, 54–66. <https://doi.org/10.1016/j.epsl.2015.01.017>
- Li, Y., Vočadlo, L., & Brodholt, J. P. (2018). The elastic properties of hcp-Fe alloys under the conditions of the Earth's inner core. *Earth and Planetary Science Letters*, 493, 118–127. <https://doi.org/10.1016/j.epsl.2018.04.013>
- Malavergne, V., Bureau, H., Raepsaet, C., Gaillard, F., Poncet, M., Surblé, S., et al. (2019). Experimental constraints on the fate of H and C during planetary core–mantle differentiation. Implications for the Earth. *Icarus*, 321, 473–485. <https://doi.org/10.1016/j.icarus.2018.11.027>
- Mashino, I., Miozzi, F., Hirose, K., Morard, G., & Sinmyo, R. (2019). Melting experiments on the Fe–C binary system up to 255 GPa: Constraints on the carbon content in the Earth's core. *Earth and Planetary Science Letters*, 515, 135–144. <https://doi.org/10.1016/j.epsl.2019.03.020>
- Morard, G., Andraut, D., Antonangeli, D., Nakajima, Y., Auzende, A. L., Boulard, E., et al. (2017). Fe–FeO and Fe–Fe₃C melting relations at Earth's core–mantle boundary conditions: Implications for a volatile-rich or oxygen-rich core. *Earth and Planetary Science Letters*, 473, 94–103. <https://doi.org/10.1016/j.epsl.2017.05.024>
- Morard, G., Andraut, D., Guignot, N., Siebert, J., Garbarino, G., & Antonangeli, D. (2011). Melting of Fe–Ni–Si and Fe–Ni–S alloys at megabar pressures: Implications for the core–mantle boundary temperature. *Physics and Chemistry of Minerals*, 373(10), 169–178. <https://doi.org/10.1016/j.epsl.2013.04.040>
- Mori, Y., Ozawa, H., Hirose, K., Sinmyo, R., Tateno, S., Morard, G., & Ohishi, Y. (2017). Melting experiments on Fe–Fe 3 S system to 254 GPa. *Earth and Planetary Science Letters*, 464, 135–141. <https://doi.org/10.1016/j.epsl.2017.02.021>
- Nakajima, Y., Imada, S., Hirose, K., Komabayashi, T., Ozawa, H., Tateno, S., et al. (2015). Carbon-depleted outer core revealed by sound velocity measurements of liquid iron–carbon alloy. *Nature Communications*, 6(1), 8942–8947. <https://doi.org/10.1038/ncomms9942>
- Narygina, O., Dubrovinsky, L. S., McCammon, C. A., Kurnosov, A., Kantor, I. Y., Prakapenka, V. B., & Dubrovinskaya, N. A. (2011). X-ray diffraction and Mössbauer spectroscopy study of FCC iron hydride FeH at high pressures and implications for the composition of the Earth's core. *Earth and Planetary Science Letters*, 307(3–4), 409–414. <https://doi.org/10.1016/j.epsl.2011.05.015>
- Nomura, R., Hirose, K., Uesugi, K., Ohishi, Y., Tsuchiyama, A., Miyake, A., & Ueno, Y. (2014). Low core–mantle boundary temperature inferred from the solidus of pyrolite. *Science*, 343(6170), 522–525. <https://doi.org/10.1126/science.1248186>
- Ohta, K., Suehiro, S., Hirose, K., & Ohishi, Y. (2018). Electrical resistivity of fcc phase iron hydrides at high pressures and temperatures. *Comptes Rendus Geoscience*, 351(2–3), 147–153. <https://doi.org/10.1016/j.crte.2018.05.004>
- Okuchi, T. (1997). Hydrogen partitioning into molten iron at high pressure: Implications for Earth's core. *Science*, 278(5344), 1781–1784. <https://doi.org/10.1126/science.278.5344.1781>
- O'Neill, H. S. C., Canil, D., & Rubie, D. C. (1998). Oxide–metal equilibria to 2500 °C and 25 GPa: Implications for core formation and the light component in the Earth's core. *Journal of Geophysical Research*, 103(B6), 12,239–12,260. <https://doi.org/10.1029/97JB02601>
- Pépin, C. M., Dewaele, A., Geneste, G., Loubeyre, P., & Mezouar, M. (2014). New iron hydrides under high pressure. *Physical Review Letters*, 113(26), 265504. <https://doi.org/10.1103/PhysRevLett.113.265504>
- Poirier, J. P. (1994). Light elements in the Earth's outer core: A critical review. *Physics of the Earth and Planetary Interiors*, 85(3–4), 319–337. [https://doi.org/10.1016/0031-9201\(94\)90120-1](https://doi.org/10.1016/0031-9201(94)90120-1)

- Sakamaki, K., Takahashi, E., Nakajima, Y., Nishihara, Y., Funakoshi, K., Suzuki, T., & Fukai, Y. (2009). Melting phase relation of FeHx up to 20 GPa: Implication for the temperature of the Earth's core. *Physics of the Earth and Planetary Interiors*, 174(1-4), 192–201. <https://doi.org/10.1016/j.pepi.2008.05.017>
- Sanloup, C., & Fei, Y. (2004). Closure of the Fe–S–Si liquid miscibility gap at high pressure. *Physics of the Earth and Planetary Interiors*, 147(1), 57–65. <https://doi.org/10.1016/j.pepi.2004.06.008>
- Sata, N., Hirose, K., Shen, G., Nakajima, Y., Ohishi, Y., & Hirao, N. (2010). Compression of FeSi, Fe₃C, Fe_{0.95}O, and FeS under the core pressures and implication for light element in the Earth's core. *Journal of Geophysical Research*, 115, B09204. <https://doi.org/10.1029/2009JB006975>
- Sato, T., Okuzumi, S., & Ida, S. (2016). On the water delivery to terrestrial embryos by ice pebble accretion. *Astronomy & Astrophysics*, 589, A15. <https://doi.org/10.1051/0004-6361/201527069>
- Shibazaki, Y., Terasaki, H., Ohtani, E., Tateyama, R., Nishida, K., Funakoshi, K., & Higo, Y. (2014). High-pressure and high-temperature phase diagram for Fe_{0.9}Ni_{0.1}–H alloy. *Physics of the Earth and Planetary Interiors*, 228, 192–201. <https://doi.org/10.1016/j.pepi.2013.12.013>
- Siebert, J., Badro, J., Antonangeli, D., & Ryerson, F. J. (2013). Terrestrial accretion under oxidizing conditions. *Science*, 339(6124), 1194–1197. <https://doi.org/10.1126/science.1227923>
- Takahashi, S., Ohtani, E., Terasaki, H., Ito, Y., Shibazaki, Y., Ishii, M., et al. (2013). Phase relations in the carbon-saturated C–Mg–Fe–Si–O system and C and Si solubility in liquid Fe at high pressure and temperature: implications for planetary interiors. *Physics and Chemistry of Minerals*, 40(8), 647–657. <https://doi.org/10.1007/s00269-013-0600-x>
- Terasaki, H., Ohtani, E., Sakai, T., Kamada, S., Asanuma, H., Shibazaki, Y., et al. (2012). Stability of Fe–Ni hydride after the reaction between Fe–Ni alloy and hydrous phase (d-AlOOH) up to 1.2 Mbar: Possibility of H contribution to the core density deficit. *Physics of the Earth and Planetary Interiors*, 194, 18–24. <https://doi.org/10.1016/j.pepi.2012.01.002>
- Terasaki, H., Shibazaki, Y., Nishida, K., Tateyama, R., Takahashi, S., Ishii, M., et al. (2014). Repulsive nature for hydrogen incorporation to Fe₃C up to 14 GPa. *ISIJ International*, 54(11), 2637–2642. <https://doi.org/10.2355/isijinternational.54.2637>
- Thompson, E. C., Davis, A. H., Bi, W., Zhao, J., Alp, E. E., Zhang, D., et al. (2018). High-pressure geophysical properties of FCC phase FeH_x. *Geochemistry, Geophysics, Geosystems*, 19, 305–314. <https://doi.org/10.1002/2017GC007168>
- Umamoto, K., & Hirose, K. (2015). Liquid iron-hydrogen alloys at outer core conditions by first-principles calculations. *Geophysical Research Letters*, 42, 7513–7520. <https://doi.org/10.1002/2015GL065899>
- Urakawa, S., Kato, M., & Kumazawa, M. (1987). Experimental study on the phase relations in the system Fe–Ni–O–S up to 15 GPa. In M. H. Manghnani & Y. Shono (Eds.), *High-Pressure Research in Mineral Physics: A Volume in Honor of Syun-iti Akimoto* (pp. 95–111). Tokyo: Terrapub/). Washington, DC: AGU. <https://doi.org/10.1029/GM039p0095>
- Walsh, K. J., Morbidelli, A., Raymond, S. N., O'Brien, D. P., & Mandell, A. M. (2011). A low mass for Mars from Jupiter's early gas-driven migration. *Nature*, 475(7355), 206–209. <https://doi.org/10.1038/nature10201>